## Evidence of an interband $\pi$ -like plasmon in silicene grown on silver

A. Sindona,<sup>1,2,\*</sup> A. Cupolillo,<sup>1,2,†</sup> F. Alessandro,<sup>1</sup> M. Pisarra,<sup>3</sup> D. C. Coello Fiallos,<sup>1</sup> S. M. Osman,<sup>1</sup> and L. S. Caputi<sup>1</sup>

Dip. di Fisica, Università della Calabria, Via P. Bucci, Cubo 30C, I-87036 Rende (CS), Italy
 INFN, sezione LNF, Gruppo collegato di Cosenza, Cubo 31C, I-87036 Rende (CS), Italy
 Dept. de Química, Univ. Autónoma de Madrid, C/ Fco. Tomás y Valiente 7, E-28049 Madrid, Spain

Silicene, the silicon-equivalent of graphene with enhanced compatibility with existing semiconductor technology, is at the heart of experimental and theoretical research on atomically thin materials that share with graphene many of its unique properties, the most remarkable of which is perhaps the Dirac-cone structure giving massless charge-carriers at the Fermi energy. Notwithstanding the predicted stability of a buckled honeycomb structure of silicon atoms in freestanding form, practical efforts on isolating a silicene sheet are most commonly focused on depositing silicon on top of silver (by epitaxial growth), where the fascinating properties of ideal silicene are substantially modified by its interaction with the supporting substrate. Indeed, studies to date on different silicene superstructures grown on Ag(111) suggest that strong hybridization occurs between the (sp)valence states of the silicon and silver atoms that may destroy not only the Dirac cone but the whole semimetallic bands of freestanding silicene. Furthermore, experimental signatures of Dirac cones in silicene/Ag(111) have been (re)interpreted as deriving from the bulk states of the substrate or the hybridized states of the interface, which has raised several thoughtful questions about the concrete possibility to use currently synthesized silicene as a platform for novel applications based on two-dimensional silicon systems. Here, we provide an unprecedented evidence that a mixed phase of silicene on Ag(111) preserves at least part of the semimetallic band structure of the unsupported silicene overlayer. In particular, we present an electron energy loss characterization of the  $\pi$ -like plasmon of silicene, which, in this multiphase geometry, survives the interaction with the silver substrate and is perfectly reproduced by ab initio calculations of the dielectric response of ideal silicene. We, therefore, propose to move the focus of interests on epitaxial growth of multiphase silicene on Ag(111), where the apparently weakened interaction with the substrate may allow to engineer or functionalize silicene as a complementary material to graphene.

Keywords: Silicene; Surface Plasmons; Electron Energy Loss Spectroscopy; Time Dependent Density Functional Theory

\*A. S. and †A. C. contributed equally

Following isolation of graphene sheets by mechanical exfoliation of its parent crystal graphite [1], an enormous effort has been directed towards two-dimensional (2D) crystals made of group-IV elements other than Carbon. A particularly noteworthy example is silicene, the silicon-equivalent of graphene with a natural compatibility with current semiconductor technology [2]-[6].

On the theoretical side, first-principles calculations of the structural properties of freestanding silicene report an intrinsic stability of a honeycomb arrangement of Si atoms in slightly buckled form, with mixed sp<sup>2</sup>-sp<sup>3</sup> hybridization [2, 7–10]. This system presents a graphene-like, semimetallic electronic structure, characterized by linearly dispersing  $\pi$  and  $\pi^*$  bands around the Fermi energy, which allows the existence of charge-carriers behaving as massless Dirac fermions [6]-[10]. Unlike graphene, freestanding silicene has a large spin-orbit coupling, which would make it suitable for valley-spintronic applications [11, 12], and an electrically, magnetically or chemically tunable band gap [13]-[17], which, for example, would allow engineering on-off current ratios and charge-carrier mobility in silicene field-effect transistors.

From the experimental point of view, silicene-like nanostructures are synthesized by epitaxial growth of silicon on silver surfaces, such as Ag(001) [18], Ag(110) [19] and Ag(111) [20], and other metal substrates, like  $ZrB_2(0001)$  [21] or Ir(111) [22]. In particular, a number of well-ordered domains have been observed on Ag(111), the formation and co-existence of which depend on the substrate temperature, during silicon growth, and the silicon deposition rate [20]-[24]. Most of these domains have a crystalline morphology being closely commensurate with the  $(4 \times 4)$ ,  $(2\sqrt{3} \times 2\sqrt{3})$  R30°,  $(\sqrt{13} \times \sqrt{13})$  R13.9° and  $(\sqrt{7} \times \sqrt{7}) \text{ R}19.1^{\circ} \text{ phases of Ag}(111) [20]-[38]. \text{ Here, the}$ different orientations, out-of-plane atomic bucklings and lattice constants of the Si atoms are reflected in markedly distinct electronic properties of the silicene overlayer, which, even without the supporting Ag substrate below, may or may not preserve the Dirac cone of its  $(1 \times 1)$ freestanding form [35, 36].

As for the interaction with Ag(111), silicene seems to lose this peculiar feature at least in the  $(4 \times 4)$  and  $(2\sqrt{3} \times 2\sqrt{3})$  R30° phases, as confirmed by angular-resolved photoemission spectroscopy (ARPES) measurements combined with density functional calculations [32]-[39]. Nonetheless, some evidences indicate that a form of Dirac cone may exist in the  $(4 \times 4)$  phase [6, 31, 40] and originate from the s-p states of bulk Ag or the strongly

hybridized sp states of Ag and Si [40]. Even in this latter case, however, the peculiar properties of freestanding silicene are destroyed by its interaction with Ag, and the transfer of the silicene to other substrates would be impractical. The major goal of silicene technology is still to grow a honeycomb-like structure of Si atoms, which preserves the semimetallic  $\pi$  and  $\pi^*$  bands.

Rather than looking at the band structure of silicene on Ag(111), here we consider exploring the intrinsic plasmonics of the interface, i.e., the coherent charge-density oscillations of its valence electrons (plasmons) excited by incident electrons or absorbed photons. In particular, we present an electron energy loss spectroscopy (EELS) characterization of a mixed phase of silicene on Ag(111), involving the  $(4 \times 4)$ ,  $(2\sqrt{3} \times 2\sqrt{3})$  R30° and  $(\sqrt{13} \times \sqrt{13})$  R13.9° superstructures, whose (optimized) geome-

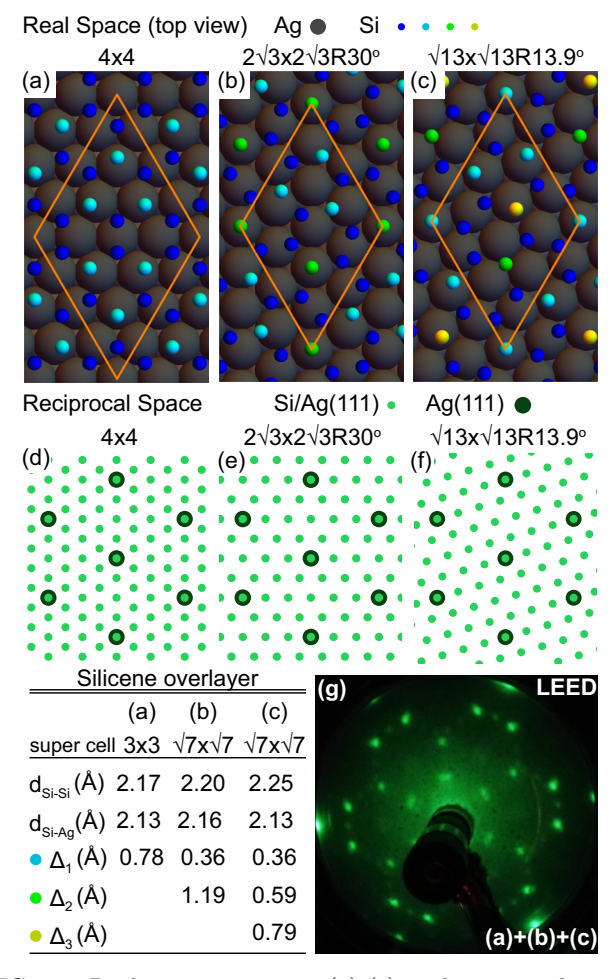


FIG. 1. Real-space geometry (a)-(c) and reciprocal space (d)-(f) of the three domains concurring to the LEED pattern in (g), which corresponds to a mixed phase of the (4×4) [(a),(d)],  $(2\sqrt{3}\times2\sqrt{3})$  R30° [(b),(e)] and  $(\sqrt{13}\times\sqrt{13})$  R13.9° [(c),(f)] superstructures, whose unit-cells are delimited with orange lines in (a)-(c). The main geometric parameters of the silicene overlayers (commensurate supercell, average in-plane bond-length  $d_{\rm Si-Si}$ , minimum Si-Ag distance  $d_{\rm Si-Ag}$  and out-of-plane atomic buckling  $\Delta_i$ ) are taken from [35, 36].

try in real and reciprocal spaces are sketched in Fig. 1(a)-(f). We report a clear signature of the existence of the  $\pi$  and  $\pi^*$  bands of silicene, whose presence is demonstrated by a  $\pi$ -like plasmon structure, appearing in the energy loss (EL) spectrum of the system, alongside the Ag plasmon and other (minor) single-particle excitation peaks.

The measurements are consistent with time dependent (TD) density functional theory (DFT) calculations of the EL function of freestanding silicene [41], showing a well resolved loss peak at 1.75 eV for a momentum transfer of the order of  $10^{-2} \text{ Å}^{-1}$ . Such a feature is absent in the plasmon structure of each single pure phase of the above mentioned types.

These arguments are not conclusive on the possibility that the silicene overlayer preserves its natural Diraccone structure, because, for example, both the interfaces of graphene on Ni(111) and Cu(111) have a well characterized  $\pi$ -plasmon, with the Dirac cone being destroyed and preserved, respectively, by hybridization with the d-bands of the supporting substrate [42, 43]. Nevertheless, our results indicate that the  $\pi$  or  $\pi^*$  character of the first valence or conduction band of silicene grown on Ag(111) may be maintained under specific geometric conditions.

The experiments were carried out at room temperature in an ultra-high vacuum chamber (with a base pressure of  $2\times10^{-10}$  Torr), using a high-resolution electron energy loss spectrometer, equipped with two 50 mm hemispherical deflectors, as monochromator and analyzer.

The EL spectra were acquired with the incident electron beam positioned at a fixed angle  $\theta_i$  of 45° from the surface normal, having a kinetic energy  $E_i$  of 40 eV. Scattered electrons were collected at an angle  $\theta_s$  of 46° from the surface normal, with an overall energy resolution of 20 meV to optimize the signal-to-noise ratio. The angular acceptance of the analyzer was 2°.

The momentum transfer q, parallel to the surface of the sample, was estimated by the conservation of energy and in-plane momentum  $q = \sqrt{2E_i} \sin \theta_i - \sqrt{2(E_i - \omega)} \sin \theta_s$ , where  $\omega$  is the energy loss. The previous equation is reported in Hartree atomic units that will be used throughout (unless otherwise specified).

The silver substrate (a disk of about 8 mm diameter) was cleaned through several cycles of Ar<sup>+</sup> ion sputtering and annealing at 770 K, until a sharp low energy electron diffraction (LEED) pattern showed the achievement of a clean and well-ordered Ag(111) surface. The deposition of Si was carried out by direct heating of a piece of Si wafer placed in front of the sample. The uptake of Si was monitored by xray photoelectron spectroscopy (XPS) and LEED.

Fig. 1(g) shows the LEED image, obtained after the deposition of silicon atoms on Ag(111) kept at 270°C. The diffraction pattern can be interpreted as originating from a mixture of the  $(4 \times 4)$ ,  $(2\sqrt{3} \times 2\sqrt{3})$  R30° and  $(\sqrt{13} \times \sqrt{13})$  R13.9° phases, similarly to what observed in [19].

Fig. 2 shows the EL spectra in the energy loss range below 6 eV, obtained from: (i) clean Ag(111) (ii) the pure  $(2\sqrt{3}\times2\sqrt{3})$  R30° phase and (iii) the mixed phase with the LEED pattern of Fig. 1(g). A prominent feature, located at about 3.8 eV, which corresponds to the surface plasmon of Ag(111), dominates all spectra. On the other hand, the Si/Ag(111) spectrum shows an additional loss located at about 0.70 eV in the pure phase and 1.75 eV in the mixed phase. The excitation energy of this mode in the mixed phase is comparable to the energy of the  $\pi$ -like plasmon calculated for intrinsic silicene in freestanding form [41]. Such a structure is absent in the EL spectrum of the  $(2\sqrt{3}\times2\sqrt{3})$  R30° phase, whereas a hybridized Si-Ag plasmon appears at lower energies.

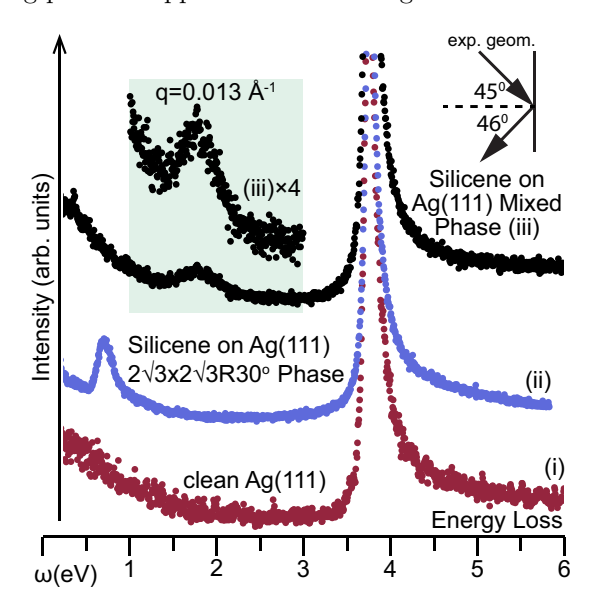


FIG. 2. EL spectra acquired from: (i) clean Ag(111) (ii) silicene on Ag(111) in the pure  $(2\sqrt{3}\times2\sqrt{3})$  R30° phase and (iii) silicene on Ag(111) in the mixed  $(4\times4)+(2\sqrt{3}\times2\sqrt{3})$  R30°+ $(\sqrt{13}\times\sqrt{13})$  R13.9° phase. In (iii), the  $\pi$ -like plasmon peak has a resonance energy of 1.70 eV associated to a transferred (in-plane) momentum of  $\sim 10^{-2}$  Å<sup>-1</sup>.

To support this observation, we used TDDFT in the random phase approximation (RPA) and computed the dielectric properties of  $(1 \times 1)$  silicene [41] in comparison with the  $(3 \times 3)$  and  $(\sqrt{7} \times \sqrt{7})$  overlayers of silicene, peeled from the silver substrate in the  $(4 \times 4)$  and  $(2\sqrt{3} \times 2\sqrt{3})$  R30° phases, respectively. The two superstructures are instructive examples of monolayer silicene, which, without the Ag substrate, would not and would preserve the Dirac-cone features, respectively [Fig. 3(a) and 3(b)].

As is customary in TDDFT [44], we started with a calculation of the ground-state electronic properties of the silicene systems, using plane-wave (PW) DFT [45], within the local density approximation (LDA) [46] and eliminating the core electrons by suitable norm-conserving pseudo-potentials [47]. Working in the Kohn-Sham (KS) formalism [48], we selected a

plane-wave (PW) basis set, within an energy cutoff of 25 Hartrees, to represent the valence electron states  $|\nu \mathbf{k}\rangle$ , associated to the band energies  $\varepsilon_{\nu \mathbf{k}}$  and labelled by the band index  $\nu$ , plus the wave vectors **k** in the first Brillouin Zone (1st BZ). As for the bulk geometry, inherent to PW-DFT, we replicated the silicene slabs with an outof-plane vacuum distance of 25 Å, to avoid overlap of charge densities located at the different replicas. Geometry optimization was performed on unsupported  $(1 \times 1)$ silicene, as in [41], and supported silicene on four Ag(111) layers, in the  $(4 \times 4)$  and  $(2\sqrt{3} \times 2\sqrt{3})$  R30° phases. In the latter case, we started from the optimized configurations of [35, 36], and relaxed the positions of all Si and Ag atoms of the topmost and second layers, respectively. A Γ-centered Monkhorst-Pack (MP) grid [49] of  $12\times12\times1$  **k**-points in the 1<sup>st</sup> BZ was used to represent the occupied and the first few empty band-states of the systems. Single-point self-consistent runs were carried out on a finer MP mesh of  $60\times60\times1$  k-points, by removing the silver layers and keeping the same optimized positions for the Si atoms as the geometry optimization step. Subsequently, the converged electron densities were used, in non-self-consistent runs, to obtain the eigensystem  $(|\nu \mathbf{k}\rangle, \varepsilon_{\nu \mathbf{k}})$  on highly resolved grids of  $240 \times 240 \times 1$ points, for  $(1 \times 1)$  silicene, and  $90 \times 90 \times 1$  points for  $(3 \times 3)$ and  $(\sqrt{7} \times \sqrt{7})$  silicene. A number of empty bands cover-

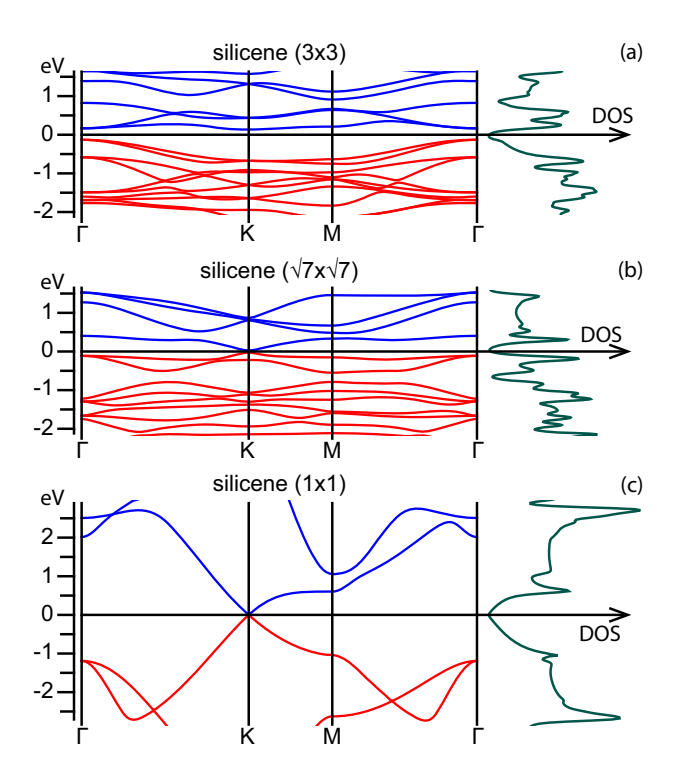


FIG. 3. Band structure (with the Fermi energy set to zero) and DOS (with a Lorentzian broadening of 0.05eV) for  $(3\times3)$  silicene (a),  $(\sqrt{7}\times\sqrt{7})$  silicene (b) and  $(1\times1)$  silicene (c). The high symmetry points  $(\Gamma, K, M)$  of the superstructures in panels (a) and (b), without the Ag substrate, are defined in the reciprocal spaces of Fig. 1(d) and 1(f), respectively

ing the KS energy spectrum up to  $15~{\rm eV}$ , above the Fermi energy, was selected in all non-self-consistent cases, to accurately describe the systems' plasmonics at energy losses below  $6~{\rm eV}$ .

The electronic structure and density of states (DOS) of our DFT+LDA computations are reported in Fig. 3, with the band energies represented along the high-symmetry path denoted  $\Gamma KM\Gamma$ . Here, we spot some peculiar features already recognized in previous studies [35, 36, 41].  $(3 \times 3)$  silicene has no Dirac cone features at K and presents a direct gap at  $\Gamma$  of 0.26 eV, between two couples of nearly degenerate states of leading  $\sigma$  and  $\pi$  symmetries, respectively [Fig. 3(a)].  $(\sqrt{7} \times \sqrt{7})$  silicene preserves a quasi linear  $\pi$ -like dispersion in the first valence and conduction bands at K, i.e., a Dirac cone with a tiny band gap of 54 meV. Freestanding  $(1 \times 1)$  silicene has two quasi-metallic bands, of dominant  $\pi$  character, whose dispersions look like the  $\pi$  bands of graphene on a reduced energy scale and with a smaller Fermi velocity value at the Dirac cone [41]. Interestingly enough,  $(\sqrt{7} \times \sqrt{7})$  and  $(1 \times 1)$  silicene have two high-dos peaks, which support electron excitations between the first valence and conduction bands near the Fermi energy, in a region of the 1<sup>st</sup>-BZ where the two  $\pi$ -like bands are quasi flat, and may assist a  $\pi$ -like plasmon oscillation.

As a second step of the TDDFT framework, we computed the unperturbed density-density response function (or unperturbed susceptibility) of the KS electrons to an energy loss  $\omega$  and momentum transfer q from the incident electron, provided by [50, 51]

$$\chi_{\mathbf{G}\mathbf{G}'}^{0} = \frac{2}{\Omega} \sum_{\mathbf{k},\nu,\nu'} \frac{(f_{\nu\mathbf{k}} - f_{\nu'\mathbf{k}+\mathbf{q}}) \rho_{\nu\nu'}^{\mathbf{k}\mathbf{q}}(\mathbf{G}) \rho_{\nu\nu'}^{\mathbf{k}\mathbf{q}}(\mathbf{G}')^{*}}{\omega + \varepsilon_{\nu\mathbf{k}} - \varepsilon_{\nu'\mathbf{k}+\mathbf{q}} + i\eta}, \quad (1)$$

The latter includes a factor of 2 for the electron-spin, the Fermi-Dirac occupations  $f_{\nu \mathbf{k}}$  and  $f_{\nu \mathbf{k}+\mathbf{q}}$  (evaluated at room temperature) a lifetime broadening parameter  $\eta$  (set to 0.02 eV), and the density-density correlation matrix elements  $\rho_{\nu\nu'}^{\mathbf{k}\mathbf{q}}(\mathbf{G}) = \langle \nu \mathbf{k} | e^{-i(\mathbf{q}+\mathbf{G})\cdot\mathbf{r}} | \nu' \mathbf{k} + \mathbf{q} \rangle$ .

The interacting density-density response function (full susceptibility) was computed using the central equation of TDDFT  $\chi_{\mathbf{GG'}} = \chi_{\mathbf{GG'}}^0 + (\chi^0 v \chi)_{\mathbf{GG'}}$  [52]. Working the RPA, we represented the interaction matrix elements in  $\chi_{\mathbf{G}\mathbf{G}'}$  by a truncated Coulomb potential, which has been accurately designed to exclude the unphysical interaction between the silicene slab replicas in a broad range of transferred momenta across the whole 1<sup>st</sup>-BZ [53]-[55]. Accordingly, the inverse dielectric matrix was obtained as  $(\epsilon^{-1})_{\mathbf{G}\mathbf{G}'} = \delta_{\mathbf{G}\mathbf{G}'} + (v\chi)_{\mathbf{G}\mathbf{G}'}$  and the EL function was calculated from the macroscopic average  $E_{\text{LOSS}} = -\text{Im}[(\epsilon^{-1})_{00}]$ . Non-local field effects [56] were included in  $E_{\text{LOSS}}$  through a dimensional cut-off on the central equation of TDDFT, which we verified to converge by reduction to a  $60 \times 60$  matrix equation, including the smallest **G**-vectors sorted in length from 0 to  $\sim 1.5 \text{Å}^{-1}$ .

In Fig. 4(a), we compare the theoretical loss spectra

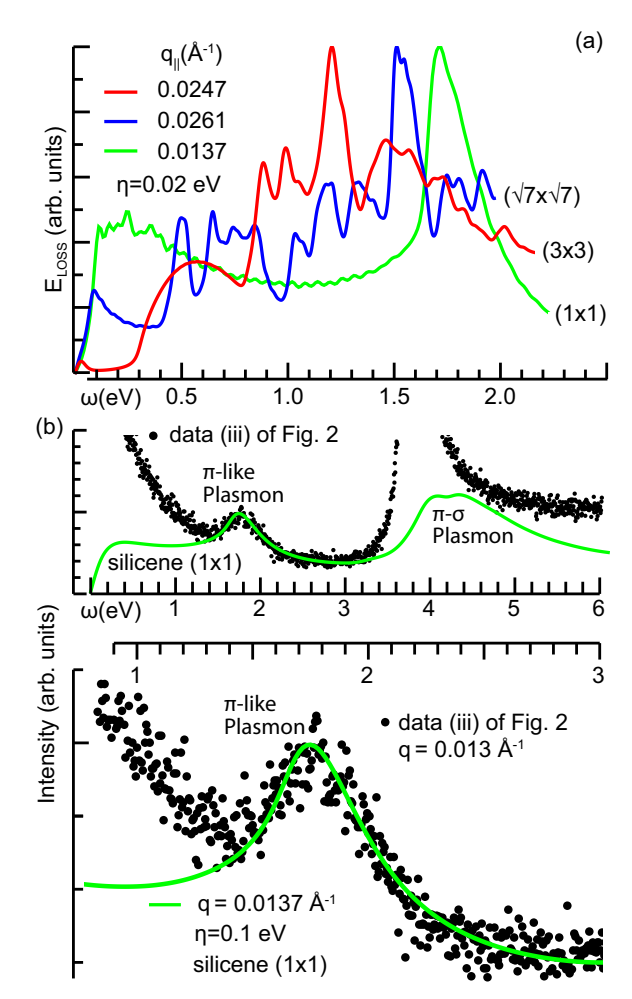


FIG. 4. (a) Theoretical loss function of  $(3\times3)$ ,  $(\sqrt{7}\times\sqrt{7})$  and  $(1\times1)$  silicene, computed with the TDFT+RPA machinery illustrated in the text. (b) Theoretical loss function of  $(1\times1)$  silicene and experimental loss spectrum (iii) of Fig. 2. In (a), small momentum transfers  $q<0.03~\text{Å}^{-1}$  are chosen in an energy loss range below 2.5 eV, with a typical lifetime broadening of 0.02 eV [in Eq. 1]. In (b), the closest simulated value of q to the experimental estimate of 0.013 Å<sup>-1</sup> is chosen for the theoretical loss curve, with an overall broadening of 0.1 eV, to cope with experimental uncertainties.

due to  $(3\times3)$ ,  $(\sqrt{7}\times\sqrt{7})$  and  $(1\times1)$  silicene, at fixed small momentum transfers parallel to  $\Gamma K$  in an energy loss range below 3 eV. The  $(3\times3)$  and  $(\sqrt{7}\times\sqrt{7})$  superstructures present a sequence of peaks generated by quasivertical electron excitations between high-dos points of the corresponding valence and conduction bands [Fig. 3(a) and 3(b)], while  $(1\times1)$  silicene has a broad primary  $\pi$ -like plasmon peak superimposed to secondary one-electron excitation structures. Of particular significance are the low energy features at  $\omega$ =0.8-1.3 eV, for  $(3\times3)$  silicene, and  $\omega$ =0.4-0.9 eV, for  $(\sqrt{7}\times\sqrt{7})$  silicene, because the associated plasmon modes appear not to be completely erased by the interaction with Ag(111). Indeed, the experimental loss of the pure  $(2\sqrt{3}\times2\sqrt{3})$  R30° phase [spectrum (ii) in Fig. 2] shows a peak, which is

consistent with the low energy end of the theoretical loss function of  $(\sqrt{7} \times \sqrt{7})$  silicene. The interaction with silver destroys the high energy loss properties of the peeled phase, and distort the low energy peak, which we attribute to a hybridized Si-Ag plasmon that keeps trace of the peeled phase. On the contrary, no signature of an interband plasmon at  $\omega=1.7-2$  eV appears in the theoretical loss spectrum of the pure phases.

In Fig. 4(b),  $(1 \times 1)$  silicene calculations are compared with the EL measurements on the coexisting silicene/Ag(111) phases [loss curve (iii) in Fig 2]. The excellent agreement, at energy losses below 3 eV, let us conclude that this mixed phase indeed present a dielectric response that matches what is expected for the  $\pi$ like plasmon of ideal silicene. Also interesting to notice is that the  $\pi$ - $\sigma$  plasmon of  $(1 \times 1)$  silicene may be present as well, though it is hidden by the Ag plasmon of the interface, as verified by comparing the loss spectrum of the mixed phase with that of clean Ag(111) [(i) in Fig. 2]. Hence, the interaction between the pure phases seem to weaken the hybridization of Si and Ag states, merging the different buckling levels of supported silicene into a configuration that resembles that of freestanding silicene. This interpretation awaits further experimental and theoretical confirmations.

In conclusion, we have examined the growth of silicene on a silver substrate, with focus on the simultaneous formation of different phases and the conditions for their coexistence. We have shown, by a combined experimental (EELS) and theoretical (TDDFT) approach, that silicene grown in a mixed phase on Ag(111) preserves at least part of the semi-metallic character of its freestanding form. On the other hand, recent progress on the epitaxial synthesis of pure, single phases of silicene on Ag(111), supported by density functional calculation of its electronic properties, indicate that strong hybridization effects make it difficult to isolate a silicene structure with well-defined quasi-metallic properties. Our proposal is then to shift the efforts of making silicene a feasible two-dimensional nanomaterial beyond graphene on epitaxial growth of silicene in mixed domains.

- \* antonello.sindona@fis.unical.it
- $^{\dagger}~anna.cupolillo@fis.unical.it$ 
  - A. S. acknowledges the computing facilities provided by the CINECA Consortium, within the INF16\_npqcd project, under the CINECA-INFN agreement.
- K. S. Novoselov, A. K. Geim, S. V. Morozov, D. Jiang, Y. Zhang, S. V. Dubonos, I. V. Grigorieva, A. A. Firsov, Science 306, 666 (2004)
- [2] K. Takeda and K. Shiraishi, Phys. Rev. B 50, 14916 (1994)
- [3] P. De Padova, P. Perfetti, B. Olivieri, C. Quaresima, C. Ottaviani, and G. Le Lay, J. Phys.: Condens. Matter 24, 223001 (2012)

- [4] A. Kara, H. Enriquez, A.P. Seitsonen, L. C. Lew Y. Voon, S. Vizzini, B. Aufray, and H. Oughaddou, Surf. Sci. Rep. 67, 1 (2012)
- [5] P. Vogt, P. De Padova, C. Quaresima, J. Avila, E. Frantzeskakis, M. C. Asensio, A. Resta, B. Ealet, and G. Le Lay, Phys. Rev. Lett. 108, 155501 (2012)
- [6] G.G. Guzman-Verri and L. C. Lew Yan Voon, Phys. Rev. B 76, 075131 (2007)
- [7] S. Cahangirov, M. Topsakal, E. Akturk, H. Sahin, and S. Ciraci, Phys. Rev. Lett. 102, 236804 (2009)
- [8] S. Cahangirov, H. Sahin, G. Le Lay, A. Rubio, "Introduction to the Physics of Silicene and other 2D Materials", Lecture Notes in Physics, Springer (2017)
- [9] S. Lebègue, O. Eriksson, Phys. Rev. B 79, 115409 (2009)
- [10] L. C. Lew Yan Voon, E. Sandberg, R.S. Aga, A.A. Farajian, Appl. Phys. Lett. 97, 163114 (2010)
- [11] C.-C. Liu, W. Feng, Y. Yao, Phys. Rev. Lett. 107, 076802 (2011)
- [12] H. Pan, Z. Li, C.-C. Liu, G. Zhu, Z. Qiao, and Y. Yao, Phys. Rev. Lett. 112, 106802 (2014)
- [13] Z. Ni, Q. Liu, K. Tang, J. Zheng, J. Zhou, R. Qin, Z. Gao, D. Yu, and J. Lu, Nano Lett. 12, 113 (2011)
- [14] T. H. Osborn, A. A. Farajian, O. V. Pupysheva, R. S. Aga, and L. L. Y. Voon, Chem. Phys. Lett. 511, 101 (2011)
- [15] N. D. Drummond, V. Zólyomi, V. I. Fal'ko, Phys. Rev. B. 85, 075423 (2012)
- [16] C. J. Tabert and E. J. Nicol, Phys. Rev. B 89, 195410 (2014)
- [17] S. Trivedi, A. Srivastava, and R. Kurchania, J. Comput. Theor. Nanosci. 11, 781 (2014)
- [18] C. Léandri, H. Oughaddou, B. Aufray, J.M. Gay, G. Le Lay, A. Ranguis, Y. Garreau, Surf. Sci. 601, 262 (2007)
- [19] B. Aufray, A. Kara, S. Vizzini, H. Oughaddou, C. Léandri, B. Ealet, G. Le Lay, Appl. Phys. Lett. 96, 183102 (2010)
- [20] B. Lalmi, H. Oughaddou, H. Enriquez, A. Kara, S. Vizzini, B. E alet, B. Aufray, Appl. Phys. Lett. 97, 223109 (2010)
- [21] A. Fleurence, R. Friedlein, T. Ozaki, H. Kawai, Y. Wang and Y. Yamada-Takamura, Phys. Rev. Lett. 108 245501 (2012)
- [22] L. Meng, Y. Wang, L. Zhang, S. Du, R. Wu, L. Li, Y. Zhang, G. Li, H. Zhou, W. A. Hofer, M. J. Gao, Nano Lett. 13 685 (2013)
- [23] C.-L. Lin, R. Arafune, K. Kawahara, N. Tsukahara, E. Minamitani, Y. Kim, N. Takagi, and M. Kawai, Appl. Phys. Expr. 5, 45802 (2012)
- [24] H. Jamgotchian, Y. Colignon, N. Hamzaoui, B. Ealet, J.Y. Hoarau, B. Aufray, and J.P. Biberian, J. Phys.: Condens. Matter 24, 172001 (2012)
- [25] Z. Majzik, M.R. Tchalala, M. Svec, P. Hapala, H. Enriquez, A. Kara, A.J. Mayne, G. Dujardin, P. Jelinek, and H. Oughaddou, J. Phys.: Condens. Matter 25, 225301 (2013)
- [26] P. Moras, T.O. Mentes, P.M. Sheverdyaeva, A. Locatelli, and C. Carbone, J. Phys.: Condens. Matter 26, 185001 (2014)
- [27] A. Acun, B. Poelsema, H.J.W. Zandvliet, and R. van Gastel, Appl. Phys. Lett. 103, 263119 (2013)
- [28] R. Arafune, C.-L. Lin, K. Kawahara, M. Kanno, N. Tsukahara, E. Minamitani, Y. Kim, N. Takagi, and M. Kawai, Surf. Sci. 608, 297 (2013)
- [29] K. Kawahara, T. Shirasawa, R. Arafune, C.-L. Lin, T.

- Takahashi, M. Kawai, and N. Takagi, Surf. Sci. **623**, 25 (2014)
- [30] L. Chen, C.-C. Liu, B. Feng, X. He, P. Cheng, Z. Ding, S. Meng, Y. Yao, and K. Wu, Phys. Rev. Lett. 109, 056804 (2012)
- [31] H. Enriquez, S. Vizzini, A. Kara, B. Lalmi, and H. Oughaddou, J. Phys.: Condens. Matter 24, 314211 (2012)
- [32] M.R. Tchalala, H. Enriquez, H. Yildirim, A. Kara, A.J. Mayne, G. Dujardin, M. Ait Ali, and H. Oughaddou, Appl. Surf. Sci. 303, 61 (2014)
- [33] J. Avila, P. De Padova, S. Cho, I. Colambo, S. Lorcy,
  C. Quaresima, P. Vogt, A. Resta, G. Le Lay, and M. C. Asensio, J. Phys.: Condens. Matter 25, 262001 (2013);
  D. Tsoutsou, E. Xenogiannopoulou, E. Golias, P. Tsipas,
  and A. Dimoulas, Appl. Phys. Lett. 103, 231604 (2013)
- [34] C.-L. Lin, R. Arafune, K. Kawahara, M. Kanno, N. Tsukahara, E. Minamitani, Y. Kim, M. Kawai, and N. Takagi, Phys. Rev. Lett. 110, 076801 (2013)
- [35] Z.-X. Guo, S. Furuya, J. I. Iwata, and A. Oshiyama, Phys. Rev. B 87, 235435 (2013)
- [36] Z.-X. Guo, S. Furuya, J. Iwata, and A. Oshiyama, J. Phys. Soc. Jpn. 82, 063714 (2013)
- [37] Y.-P. Wang and H.-P. Cheng, Phys. Rev. B 87, 245430 (2013)
- [38] S. K. Mahatha, P. Moras, V. Bellini, P. M. Sheverdyaeva, C. Struzzi, and L. Petaccia, C. Carbone, Phys. Rev. B 89, 201416 (2014)
- [39] P. M. Sheverdyaeva, S. K. Mahatha, P. Moras, L. Petaccia, G. Fratesi, G. Onida, C. Carbone, ACS Nano 11, 07593 (2017)

- [40] Y. Feng et al, PNAS **113** (51), 14656 (2016)
- [41] C. Vacacela Gomez, M. Pisarra, M. Gravina, P. Riccardi, and A. Sindona, Phys. Rev. B 95, 085419 (2017)
- [42] A. V. Generalov and Y. S. Dedkov, Carbon 50, 183 (2012)
- [43] A. Cupolillo, N. Ligato, L. S. Caputi, Carbon 50, 2588 (2012)
- [44] M. Petersilka, U. J. Gossmann, and E. K. U. Gross, Phys. Rev. Lett. 76 1212 (1996)
- [45] X. Gonze et al., Comput. Phys. Commun. 180 2582 (2009)
- [46] J. P. Perdew and A. Zunger, Phys. Rev. B 23 5048 (1981)
- [47] N. Troullier and J. L. Martins, Phys. Rev. B 43 1993 (1991)
- [48] W. Kohn and L. J. Sham, Phys. Rev.140 A1133 (1965)
- [49] H. J. Monkhorst and J. D. Pack, Phys. Rev. B 13 5188 (1976)
- [50] S. L. Adler, Phys. Rev. 126 413 (1962)
- [51] N. Wiser, Phys. Rev. 129 69 (1963)
- [52] G. Onida, L. Reining, and A. Rubio, Rev. Mod. Phys. 74 601 (2002)
- [53] V. Despoja, K. Dekanić, M. Šunjić, L. Marušić, Phys. Rev. B 86 165419 (2012)
- [54] M. Pisarra, A. Sindona, M. Gravina, V. M. Silkin, and J. M. Pitarke Phys. Rev. B 93, 035440 (2016)
- [55] C. Vacacela Gomez, M. Pisarra, M. Gravina, J. M. Pitarke, and A. Sindona, Phys. Rev. Lett. 117, 116801 (2016)
- [56] C. Kramberger et al, Phys. Rev. Lett 100 196803 (2008)